

# Approximation of the grad div Operator in Nonconvex Domains

D. Boffi,<sup>1</sup> C. Chinosi,<sup>2</sup> L. Gastaldi<sup>3</sup>

## Abstract:

In this paper we are dealing with the approximation of the grad-div operator in nonconvex polygonal domains. A penalization strategy is considered in order to obtain a formulation of the original eigenproblem which is associated with an elliptic operator. However the presence of singular eigensolutions, in the case of nonconvex domains, is the origin of major troubles in the numerical approximation of the problem. A mixed-type approximation, based on a projection procedure, is introduced and analyzed from the theoretical and numerical point of view. Several numerical experiments confirm that in presence of singularities the projection is needed in order to reproduce the features of the continuous problem.

## 1 Introduction

Let  $\Omega$  be an open polygon, denote by  $\underline{n}$  the outward normal vector to its boundary  $\partial\Omega$ . Let us consider the following eigenproblem:

$$\begin{cases} -\underline{\text{grad}} \text{div} \underline{u} = \omega^2 \underline{u} & \text{in } \Omega \\ \text{rot} \underline{u} = 0 & \text{in } \Omega \\ \underline{u} \cdot \underline{n} = 0 & \text{on } \partial\Omega. \end{cases} \quad (1)$$

The problem above describes the vibration frequencies of a fluid in a cavity, hence it can be considered as the simplest problem in fluid-structure interaction, see e.g., Morand and Ohayon (1992).

Using standard orthogonalities in  $\mathbb{R}^2$  between the operators  $\underline{\text{grad}}$  and  $\underline{\text{curl}}$ , equation (1) can be related to a vibration problem arising in electromagnetic applications, see Boffi, Fernandes, Gastaldi, and Perugia (1996, 1999); Bermúdez and Pedreira (1992); Kikuchi (1987).

In the literature two ways are frequently used to treat numerically the constraint in problem (1). Firstly, one can observe that the constraint  $\text{rot} \underline{u} = 0$  follows automatically from the equation  $-\underline{\text{grad}} \text{div} \underline{u} = \omega^2 \underline{u}$  and the condition  $\omega \neq 0$ . Hence one can drop the irrotationality constraint and add a zero frequency corresponding to the infinite dimensional null space of the operator  $\underline{\text{grad}} \text{div}$ . Numerical methods based on this idea have been analyzed, for instance, in Kikuchi (1987);

Bermúdez and Pedreira (1992); Webb (1993); Bossavit (1990) for the Maxwell's problem and in Bermúdez, Durán, Muschiatti, Rodríguez, and Solomin (1995); Chen and Taylor (1990) for the fluid-structure example. In Boffi, Fernandes, Gastaldi, and Perugia (1999) a general analysis is presented, in order to predict the performance of a finite element scheme. This result is based on the approximation of an equivalent mixed formulation. In particular it is proved that the so-called "edge elements" (see Nédélec (1982)) work well. The same analysis shows that the so-called Raviart-Thomas elements (see Raviart and Thomas (1977)) are well-suited for problem (1) (see also Bermúdez, Durán, Muschiatti, Rodríguez, and Solomin (1995)).

The other approach consists in a penalization strategy (see, for example, Kikuchi (1987); Bathe, Nitikitpaiboon, and Wang (1995); Wang and Bathe (1997b); Gastaldi (1996)), which we are going to consider in the present paper.

We shall use the following notation: if  $\underline{v} = (v_1, v_2)$  is a vector field then  $\text{rot} \underline{v} = \frac{\partial v_2}{\partial x} - \frac{\partial v_1}{\partial y}$  and if  $\varphi$  is a scalar field  $\underline{\text{curl}} \varphi = (\frac{\partial \varphi}{\partial y}, -\frac{\partial \varphi}{\partial x})$ .

Let  $\alpha$  be a positive real number, then the penalized formulation of problem (1) reads:

$$\begin{aligned} & \text{find } \omega \in \mathbb{R} \text{ such that there exists } \underline{u} \neq 0: \\ & \begin{cases} -\underline{\text{grad}} \text{div} \underline{u} + \alpha \underline{\text{curl}} \text{rot} \underline{u} = \omega^2 \underline{u} & \text{in } \Omega \\ \underline{u} \cdot \underline{n} = 0 & \text{on } \partial\Omega \\ \text{rot} \underline{u} = 0 & \text{on } \partial\Omega. \end{cases} \end{aligned} \quad (2)$$

This problem is now associated with an elliptic operator, so that one might think that any trouble has gone away. However, this problem hides several insidious aspects as we shall see below. In particular, in the case of nonconvex domains some eigenfunctions could be singular (see Costabel and Dauge (1997)), so that one must be very careful with the choice of the correct variational formulation of (2). Consequently, the numerical scheme must be suitably constructed in order to correctly approximate the possible singular functions.

In this paper we consider the finite element scheme proposed in Bathe, Nitikitpaiboon, and Wang (1995); Wang and Bathe (1997b). The basic idea of that method consists in using a mixed three-fields formulation to impose the constraints in a weaker form. The method can actually be interpreted as a projection procedure of the bilinear form. We shall show that this method provides good approximation of problem (2) and give some indication about the analysis of the convergence.

<sup>1</sup> Dipartimento di Matematica "F. Casorati", Università di Pavia, Italy and Department of Mathematics, Pennsylvania State University, USA

<sup>2</sup> Dipartimento di Scienze e Tecnologie Avanzate, Università del Piemonte Orientale, Alessandria, Italy

<sup>3</sup> Dipartimento di Matematica, Università di Brescia, Italy

The outline of the paper is as follows. In Section 2 we introduce the problem, with particular emphasis on the singular behavior of the solution close to a reentrant corner. In Section 3 we describe the scheme and show that it is equivalent to a mixed approximation. The last section is devoted to several numerical experiments confirming the theoretical results presented before.

## 2 Setting of the problem

We shall use the following Hilbert spaces with their natural norms:

$$\begin{aligned}
L^2(\Omega) &= \{u : \Omega \rightarrow \mathbb{R} : \int_{\Omega} u^2 < \infty\} \\
L_0^2(\Omega) &= \{u \in L^2(\Omega) : \int_{\Omega} u = 0\} \\
H^1(\Omega) &= \{u \in L^2(\Omega) : \underline{\text{grad}} u \in L^2(\Omega)^2\} \\
H_0^1(\Omega) &= \{u \in H^1(\Omega) : u = 0 \text{ on } \partial\Omega\} \\
H(\text{div}; \Omega) &= \{\underline{u} \in L^2(\Omega)^2 : \text{div } \underline{u} \in L^2(\Omega)\} \\
H_0(\text{div}; \Omega) &= \{\underline{u} \in H(\text{div}; \Omega) : \underline{u} \cdot \underline{n} = 0 \text{ on } \partial\Omega\} \\
H(\text{rot}; \Omega) &= \{\underline{u} \in L^2(\Omega)^2 : \text{rot } \underline{u} \in L^2(\Omega)\} \\
H(\text{rot}^0; \Omega) &= \{\underline{u} \in L^2(\Omega)^2 : \text{rot } \underline{u} = 0 \text{ in } \Omega\}
\end{aligned} \tag{3}$$

finally,  $(\cdot, \cdot)$  denotes the scalar product in  $L^2(\Omega)$ .

A penalized variational formulation of (1) is:

$$\begin{aligned}
&\text{find } \omega \in \mathbb{R} \text{ such that there exists} \\
&\underline{u} \in H_0(\text{div}; \Omega) \cap H(\text{rot}; \Omega) \text{ with } \underline{u} \neq 0 : \\
&(\text{div } \underline{u}, \text{div } \underline{v}) + \alpha(\text{rot } \underline{u}, \text{rot } \underline{v}) = \omega^2(\underline{u}, \underline{v}) \\
&\quad \forall \underline{v} \in H_0(\text{div}; \Omega) \cap H(\text{rot}; \Omega).
\end{aligned} \tag{4}$$

The following characterization of the eigensolutions of problem (4) will be helpful for the interpretation of the numerical results in the last section, (see Costabel and Dauge (1999) for the details of the proof).

**Proposition 1** *Let  $(\omega, \underline{u})$  be an eigensolution of (4), then it belongs to one of the two following disjoint families:*

- i)  $(\kappa_N, \underline{\text{grad}} p)$  with  $(\kappa_N, p)$  eigensolutions of the following Neumann eigenproblem for the Laplace operator:

$$\begin{aligned}
-\Delta p &= \kappa_N p && \text{in } \Omega \\
\frac{\partial p}{\partial \underline{n}} &= 0 && \text{on } \partial\Omega \\
\int_{\Omega} p &= 0;
\end{aligned} \tag{5}$$

- ii)  $(\alpha\kappa_D, \underline{\text{curl}} \lambda)$  with  $(\kappa_D, \lambda)$  eigensolutions of the following Dirichlet problem

$$\begin{aligned}
-\Delta \lambda &= \kappa_D \lambda && \text{in } \Omega \\
\lambda &= 0 && \text{on } \partial\Omega.
\end{aligned} \tag{6}$$

We notice that the eigensolutions of problems (5) and (6) are related to the eigensolutions of the original problem (4) as follows:

$$\begin{aligned}
\kappa_N &= \omega^2, & p &= \text{div } \underline{u}, & \underline{u} &= -\frac{1}{\omega^2} \underline{\text{grad}} p \\
\kappa_D &= \frac{\omega^2}{\alpha}, & \lambda &= \text{rot } \underline{u}, & \underline{u} &= \frac{\alpha}{\omega^2} \underline{\text{curl}} \lambda.
\end{aligned} \tag{7}$$

The first family corresponds to those eigensolutions with  $\text{rot } \underline{u} = 0$  while the second one to those with  $\text{div } \underline{u} = 0$ . Therefore, we have that  $\text{div } \underline{u}$  and  $\text{rot } \underline{u}$  cannot be both different from zero. Moreover if  $\alpha$  is sufficiently big the first eigenvalues of (4), ordered as an increasing sequence, correspond to those of problem (5) and satisfy  $\text{rot } \underline{u} = 0$ . The frequencies corresponding to the eigensolutions  $\underline{u}$  with  $\text{div } \underline{u} = 0$  are shifted accordingly to the rule  $\omega^2 = \alpha\kappa_D$ . Suppose now to have an estimate of the smallest eigenvalue  $\kappa_D^1$  of (6). Then if one is interested in the eigenvalues  $\omega^2$  of (1) verifying  $\omega^2 < M$ , for a given  $M$ , it is sufficient to choose  $\alpha$  so that  $\alpha\kappa_D^1 > M$  and all the eigenvalues of (4) with  $\omega^2 < M$  are exactly the required eigenvalues of (1). To conclude this remark we point out that in this sense, one can consider the penalization introduced in (4) as an “exact penalization”. And in particular we do not need  $\alpha$  to be so large if we are interested only in few eigensolutions.

In Costabel and Dauge (1997) the regularity of  $\text{div } \underline{u}$  and of  $\text{rot } \underline{u}$  has also been considered. Adapting the proof to the present two-dimensional problem, one gets

**Proposition 2** *Let  $\underline{u} \in H_0(\text{div}; \Omega) \cap H(\text{rot}; \Omega)$  be an eigenfunction of problem (4) then*

$$\text{div } \underline{u} \in H^1(\Omega) \quad \text{and} \quad \text{rot } \underline{u} \in H_0^1(\Omega). \tag{8}$$

It is well-known that if  $\Omega$  is convex the space  $H_0(\text{div}; \Omega) \cap H(\text{rot}; \Omega)$  is equal to  $H^1(\Omega)^2 \cap H_0(\text{div}; \Omega)$ . Thus an equivalent variational formulation making use of the space  $H^1(\Omega)^2 \cap H_0(\text{div}; \Omega)$  can be introduced:

$$\begin{aligned}
&\text{find } \omega \in \mathbb{R} \text{ such that there exists} \\
&\underline{u} \in H^1(\Omega)^2 \cap H_0(\text{div}; \Omega) \text{ with } \underline{u} \neq 0 : \\
&(\text{div } \underline{u}, \text{div } \underline{v}) + \alpha(\text{rot } \underline{u}, \text{rot } \underline{v}) = \omega^2(\underline{u}, \underline{v}) \\
&\quad \forall \underline{v} \in H^1(\Omega)^2 \cap H_0(\text{div}; \Omega).
\end{aligned} \tag{9}$$

This equivalence fails if  $\Omega$  is a nonconvex polygon, as it has been shown in Costabel and Dauge (1997). It is well-known that (4) admits “singular” eigenfunctions which are not in  $H^1(\Omega)$ . Hence they do not satisfy problem (9); conversely not all of the  $H^1$ -solutions of (9) solve (4) and the original problem (2). Moreover the eigensolutions of (9) do not split anymore into the two disjoint families described before in Prop. 1. They depend analytically on  $\alpha$  and the following characterization holds true (see Costabel and Dauge (1999)).

**Proposition 3** *Let  $\Omega$  be a nonconvex polygon. The eigenvectors of (9) which do not depend on  $\alpha$  are the eigenvectors of (4) which belong to  $H^1(\Omega)$ .*

*Moreover, the eigensolutions tend to those of a Stokes-like problem, as  $\alpha$  goes to infinity.*

To end up the section, we observe also that the eigenfunctions of (9) do not have regular divergence and rotational, as we shall show in the numerical results reported in Section 4.

### 3 The finite element approximation

The results presented at the end of the previous section have important consequences for the numerical approximation of (4). Let  $\Sigma_h$  be a finite dimensional subspace of  $H_0(\text{div}; \Omega) \cap H(\text{rot}; \Omega)$ , then we consider the following problem:

$$\begin{aligned} \text{find } \omega_h \in \mathbb{R} \text{ such that there exists } \underline{u}_h \in \Sigma_h \text{ with } \underline{u}_h \neq 0: \\ (\text{div} \underline{u}_h, \text{div} \underline{v}_h) + \alpha(\text{rot} \underline{u}_h, \text{rot} \underline{v}_h) = \omega_h^2 (\underline{u}_h, \underline{v}_h) \\ \forall \underline{v}_h \in \Sigma_h. \end{aligned} \quad (10)$$

Indeed, if the spaces  $\Sigma_h$ , for  $h > 0$ , are made of continuous vector functions it follows that the closure of  $\cup_{h>0} \Sigma_h$  is strictly contained in  $H^1(\Omega)^2$ . This means that if  $\underline{u}$  is an eigenfunction of (4) which does not belong to  $H^1(\Omega)^2$  then it cannot be the limit as  $h$  tends to 0 of any sequence  $\{\underline{v}_h\}_{h>0}$  with  $\underline{v}_h \in \Sigma_h$ . Therefore the corresponding eigenvalue will not be correctly approximated.

On the other hand, we observe that it is not possible to construct a piecewise polynomial function  $\underline{w}$  which is contained in  $H_0(\text{div}; \Omega) \cap H(\text{rot}; \Omega)$  but not in  $H^1(\Omega)^2$ . Indeed, if  $\underline{w}$  belongs to  $H_0(\text{div}; \Omega) \cap H(\text{rot}; \Omega)$ , then both  $\text{div} \underline{w}$  and  $\text{rot} \underline{w}$  are in  $L^2(\Omega)$ . This implies that both the normal and the tangential components are continuous across the interelement boundaries, so that  $\underline{w}$  is in  $H^1(\Omega)^2$ .

**Remark 1** *Let  $\Omega$  be an L-shaped domain; consider a triangular mesh and define  $\Sigma_h$  as the space of continuous piecewise linear vector fields. Then the solutions to (10) do not approximate those of (4). Indeed, since in this case  $\Omega$  is clearly non-convex,  $H^1(\Omega)^2 \cap H_0(\text{div}; \Omega)$  is a closed proper subspace of  $H_0(\text{div}; \Omega) \cap H(\text{rot}; \Omega)$  i.e., if  $\underline{u}_h \in \Sigma_h$  and*

$$\lim_{h \rightarrow 0} (\|\underline{u}_h - \underline{u}\|_0 + \|\text{div}(\underline{u}_h - \underline{u})\|_0 + \|\text{rot}(\underline{u}_h - \underline{u})\|_0) = 0 \quad (11)$$

then

$$\underline{u} \in H^1(\Omega)^2 \cap H_0(\text{div}; \Omega). \quad (12)$$

*The eigenfunction corresponding to the first eigenvalue belongs to  $H_0(\text{div}; \Omega) \cap H(\text{rot}; \Omega) \setminus H^1(\Omega)^2 \cap H_0(\text{div}; \Omega)$  and, according to the above discussion, it cannot be approximated in the energy norm by a sequence of discrete elements in  $\Sigma_h$ . The computed eigenfunction is presented in Fig. 1. It is apparent that the singularity at the reentrant corner is completely missed.*

To avoid the inconveniences presented above, one can modify the discretization of (4) by a reduced integration procedure. With the introduction of  $L^2(\Omega)$ -projection operators  $\mathbf{P}_1$  and  $\mathbf{P}_2$  into suitable finite element subspaces  $W_h^1$  and  $W_h^2$  of  $L_0^2(\Omega)$  and  $L^2(\Omega)$  respectively, the new discrete formulation reads as

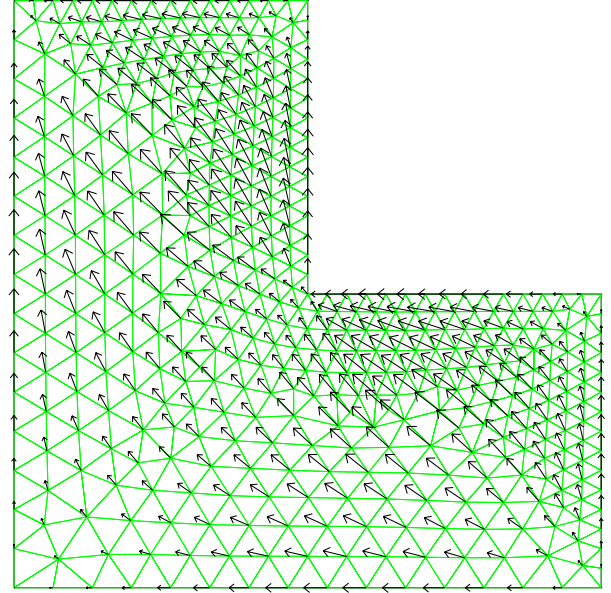


**Figure 1** : Singular eigenfunction computed wrongly by piecewise linears.

follows

$$\begin{aligned} \text{find } \omega_h \in \mathbb{R} \text{ such that there exists } \underline{u}_h \in \Sigma_h, \text{ with } \underline{u}_h \neq 0: \\ (\mathbf{P}_1 \text{div} \underline{u}_h, \mathbf{P}_1 \text{div} \underline{v}_h) + \alpha(\mathbf{P}_2 \text{rot} \underline{u}_h, \mathbf{P}_2 \text{rot} \underline{v}_h) \\ = \omega_h^2 (\underline{u}_h, \underline{v}_h) \quad \forall \underline{v}_h \in \Sigma_h. \end{aligned} \quad (13)$$

We observe that this numerical scheme can be interpreted as a finite element approximation of the so called three-fields formulation introduced in Bathe, Nitikitpaiboon, and Wang (1995); Wang and Bathe (1997b) and analyzed also in Gastaldi (1996).

We introduce suitable bilinear forms, one of them depending on the penalization parameter  $\alpha$

$$\begin{aligned} a_\alpha(\cdot, \cdot) : (L_0^2(\Omega) \times L^2(\Omega))^2 \rightarrow \mathbb{R} \\ a_\alpha((p, \lambda); (q, \mu)) = (p, q) + \frac{1}{\alpha}(\lambda, \mu), \end{aligned} \quad (14)$$

$$\begin{aligned} b(\cdot, \cdot) : H_0(\text{div}; \Omega) \cap H(\text{rot}; \Omega) \times (L_0^2(\Omega) \times L^2(\Omega)) \rightarrow \mathbb{R} \\ b(\underline{v}; (q, \mu)) = (\text{div} \underline{v}, q) + (\text{rot} \underline{v}, \mu). \end{aligned} \quad (15)$$

Consider the following problem:

$$\begin{aligned} \text{find } \kappa_h \in \mathbb{R} \text{ such that there exists a nonzero triplet} \\ (p_h, \lambda_h, \underline{w}_h) \in W_h^1 \times W_h^2 \times \Sigma_h : \\ a_\alpha((p_h, \lambda_h); (q_h, \mu_h)) + b(\underline{w}_h; (q_h, \mu_h)) = 0 \\ \forall (q_h, \mu_h) \in W_h^1 \times W_h^2 \\ b(\underline{v}_h; (p_h, \lambda_h)) = -\kappa_h^2 (\underline{w}_h, \underline{v}_h) \quad \forall \underline{v}_h \in \Sigma_h. \end{aligned} \quad (16)$$

**Proposition 4** If  $(\omega_h, \underline{u}_h) \in \mathbb{R} \times \Sigma_h$  is an eigensolution of (13), then there exists  $(p_h, \lambda_h) \in W_h^1 \times W_h^2$  such that  $(\kappa_h, p_h, \lambda_h, \underline{w}_h)$  is an eigensolution of (16) with  $\kappa_h = \omega_h$  and  $\underline{w}_h = \underline{u}_h$ . Conversely, for any solution  $(\kappa_h, p_h, \lambda_h, \underline{w}_h)$  of (16) we have that  $\omega_h = \kappa_h$  and  $\underline{u}_h = \underline{w}_h$  solve (13).

*Proof.* Let  $(\omega_h, \underline{u}_h) \in \mathbb{R} \times \Sigma_h$  be an eigensolution of (13), then let us define  $p_h = -\mathbf{P}_1 \operatorname{div} \underline{u}_h \in W_h^1$  and  $\lambda_h = -\alpha \mathbf{P}_2 \operatorname{rot} \underline{u}_h \in W_h^2$  and substitute in (13). Then the second equation in (16) holds true with  $\underline{w}_h = \underline{u}_h$  and  $\kappa_h = \omega_h$ . By definition of the bilinear forms  $a_\alpha$  and  $b$  (see (14) and (15)) and of the projection operators  $\mathbf{P}_1$  and  $\mathbf{P}_2$ , also the first equation easily follows.

Conversely, the first equation in (16) implies that  $p_h = -\mathbf{P}_1 \operatorname{div} \underline{w}_h$  and  $\lambda_h = -\alpha \mathbf{P}_2 \operatorname{rot} \underline{w}_h$  and substituting these equalities in the second equations, gives that  $\underline{u}_h = \underline{w}_h$  and  $\omega_h = \kappa_h$  satisfy (13).  $\square$

**Remark 2** By virtue of the previous proposition, in the rest of the paper we shall denote by  $\underline{u}_h$  both the solution of (13) and the last component of the solution of (16). Analogously,  $\omega_h$  will be the corresponding eigenvalue.

Following Bathe, Nitikitpaiboon, and Wang (1995); Wang and Bathe (1997b); Gastaldi (1996), given a quadrilateral decomposition of  $\Omega$ , a possible choice for the discrete spaces is:

$$\begin{aligned} \Sigma_h^1 &= \{ \underline{v} \in H(\operatorname{div}; \Omega) \cap H(\operatorname{rot}; \Omega) : \underline{v} \text{ is a continuous} \\ &\quad \text{piecewise biquadratic vector field with} \\ &\quad \text{appropriate b.c.} \}, \\ W_h^1 &= \{ q_h \in L_0^2(\Omega) : q_h \text{ is piecewise linear} \}, \\ W_h^2 &= \{ \mu_h \in L^2(\Omega) : \mu_h \text{ is piecewise linear} \}. \end{aligned} \quad (17)$$

The boundary conditions on an element  $\underline{v}$  of  $\Sigma_h^1$  are prescribed as follows. If at a node the outward normal versor  $\underline{n}$  can be defined (that is if the node lies on the interior part of a side of  $\Omega$ ) then  $\underline{v} \cdot \underline{n} = 0$ . At the nodes lying at the corners of  $\Omega$  we distinguish two possible situations. If the corner is the vertex of a convex angle of  $\Omega$  then  $\underline{v} = (0, 0)$ ; otherwise we prescribe  $\underline{v} \cdot \underline{n} = 0$  where  $\underline{n}$  is a suitably defined linear combination of the two normal vectors corresponding to the sides of the corner, according to the suggestion of Wang and Bathe (1997a). In the case of the L-shaped domain there is only one reentrant corner and we take  $\underline{n}$  along the bisecting line of the corner.

We observe that, with the choice (17),  $\omega_h = 0$  may be a spurious solution of (13) and (16), corresponding to those  $\underline{u}_h$ , such that  $(\operatorname{div} \underline{u}_h, q_h) + (\operatorname{rot} \underline{u}_h, \mu_h) = 0$  for all  $q_h \in W_h^1$  and  $\mu_h \in W_h^2$ . Let us denote by  $K_h$  this discrete nullspace. On the other hand, let  $(\omega_h, \underline{u}_h)$  be an eigensolution of (13) with  $\omega_h \neq 0$  and let us take  $\underline{v}_h \in K_h$ . Then (13) implies  $(\underline{u}_h, \underline{v}_h) = 0$ . Let us define the space  $\Sigma_h^2$  obtained by projecting  $\Sigma_h^1$  onto the orthogonal space of  $K_h$  in  $\Sigma_h$  and consider problem (13) with  $\Sigma_h = \Sigma_h^2$ . It follows that the resulting eigenvalues are strictly positive and coincides with the nonzero ones obtained with  $\Sigma_h = \Sigma_h^1$ .

Let us introduce the continuous eigenproblem corresponding to (16),

$$\begin{aligned} &\text{find } \omega \in \mathbb{R} \text{ such that there exists a nonzero triplet} \\ &(p, \lambda, \underline{u}) \in L_0^2(\Omega) \times L^2(\Omega) \times H_0(\operatorname{div}; \Omega) \cap H(\operatorname{rot}; \Omega): \\ &a_\alpha((p, \lambda); (q, \mu)) + b(\underline{u}, (q, \mu)) = 0 \\ &\quad \forall (q, \mu) \in L_0^2(\Omega) \times L^2(\Omega) \\ &b(\underline{v}, (p, \lambda)) = -\omega^2(\underline{u}, \underline{v}) \forall \underline{v} \in H_0(\operatorname{div}; \Omega) \cap H(\operatorname{rot}; \Omega). \end{aligned} \quad (18)$$

We notice that the unknown  $p$  has a physical meaning and represents the pressure of the fluid.

It is not difficult to check that (18) is equivalent to the penalized problem (4).

If we consider the *source* problem associated with (16), it is well-known that the stability property is a consequence of the ellipticity and inf-sup condition we are going to state (see Brezzi and Fortin (1991)). The convergence follows then usually from the stability and the approximation properties of the finite element spaces.

It turns out (from a numerical estimate) that the standard inf-sup condition is not satisfied in the case of a nonconvex domain. This means that not only the (continuous) finite elements are not able to capture the singularities as discussed above, but also the numerical method is not stable in the energy norm. If we replace the energy norm with the (natural) mesh dependent norm coming out from the introduction of the projections  $\mathbf{P}_1$  and  $\mathbf{P}_2$ , then the numerical inf-sup constant is bounded below away from zero.

This is not yet a proof of convergence for the *eigenvalue* problem (16) (in particular it has been shown that in order to prove the convergence of the eigenmodes we need other additional properties, see Boffi, Brezzi, and Gastaldi (1997b,a)), but suggests a possible direction for further analysis.

### 3.1 The ellipticity in the kernel property

$$a_\alpha((p_h, \lambda_h), (p_h, \lambda_h)) \geq C \|(p_h, \lambda_h)\|_0^2 \quad \forall (p_h, \lambda_h) \in W_h^1 \times W_h^2. \quad (19)$$

The previous result is an immediate consequence of the definition of the bilinear form  $a_\alpha(\cdot, \cdot)$ . The constant  $C$ , which depends on  $\alpha$  but is independent of  $h$ , is the same constant which appear in the analysis of the continuous problem (18).

### 3.2 Inf-sup condition

There exists a positive constant  $\beta$  independent of  $h$  such that

$$\inf_{\underline{u}_h \in \Sigma_h^2} \sup_{(q_h, \mu_h) \in W_h^1 \times W_h^2} \frac{b(\underline{u}_h, (q_h, \mu_h))}{\|\underline{u}_h\|_h \|(q_h, \mu_h)\|_0} \geq \beta > 0. \quad (20)$$

In (20) the mesh-dependent norm  $\|\cdot\|_h$  is defined as follows:

$$\|\underline{u}\|_h^2 = \|\underline{u}\|_0^2 + \|\mathbf{P}_1 \operatorname{div} \underline{u}\|_0^2 + \|\mathbf{P}_2 \operatorname{rot} \underline{u}\|_0^2. \quad (21)$$

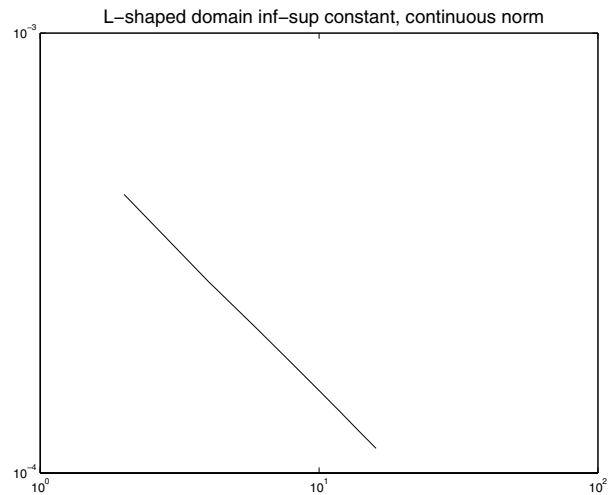
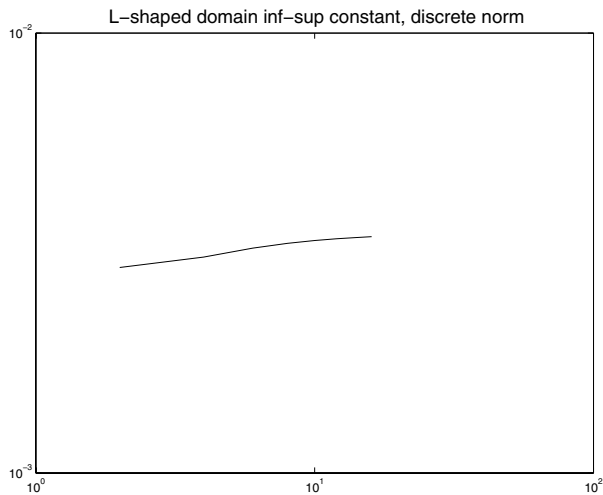
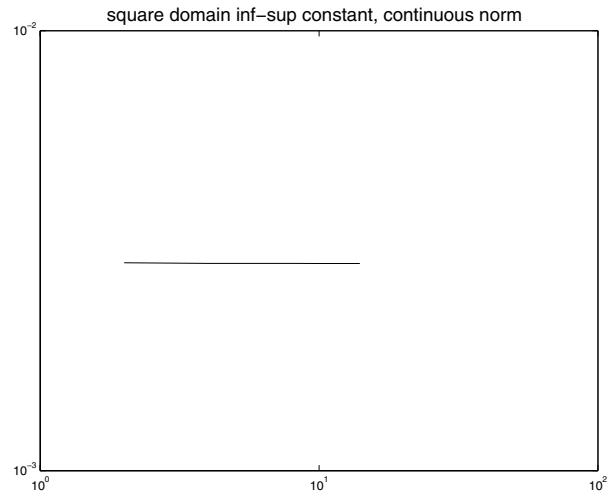
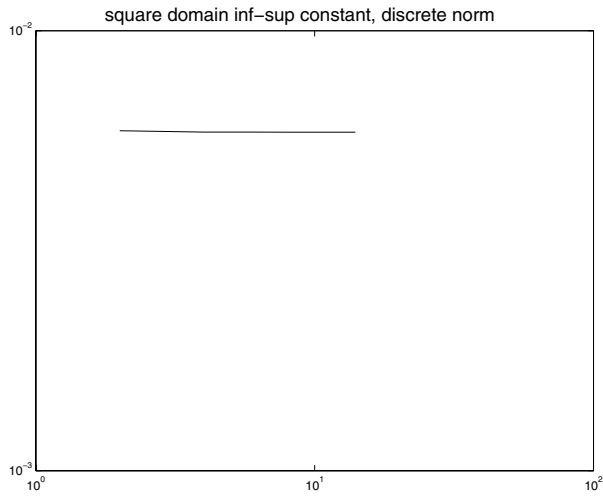


**Figure 2** : Inf-sup constant with the discrete norm: square domain (top), L-shaped domain (bottom).

**Figure 3** : Inf-sup constant with the continuous norm: square domain (top), L-shaped domain (bottom).

We do not have a complete proof of (20), however numerical results show that it is valid for both convex and nonconvex domains. In Fig. 2 the inf-sup constant  $\beta$  for different values of  $h$  has been plotted relatively to a square and an L-shaped domain. The graphs run from left to right, so we can see that in the case of reentrant corner the inf-sup constant is even increasing as  $h$  goes to zero. In Fig. 3 we consider the standard inf-sup constant where the discrete norm  $\|\cdot\|_h$  is replaced by the energy norm in  $H_0(\text{div}; \Omega) \cap H(\text{rot}; \Omega)$ . We see that when the domain is convex nothing changes, while in the case of reentrant corner the inf-sup constant tends to zero.

#### 4 Numerical results

As previously observed, when  $\Omega$  is a nonconvex polygon, problem (2) could admit eigensolutions with singularities.

These solutions are well represented if the variational formulation (4) is considered, but they do not solve problem (9). From the point of view of the approximation this behavior causes some problems. The displacement-type approximation (10) of problem (4) corresponds to an exact integration scheme and it is a conforming approximation of problem (9); the solutions of (10) cannot approximate the singular eigenfunctions, as they approximate the  $H^1$ -solutions of problem (9). To overcome these problems it has been introduced the new discrete formulation (13), based on a reduced integration procedure. In order to compare the numerical solutions of the discrete problems (10) and (13) respectively, we present in this section some numerical experiments. We consider two test problems with convex and nonconvex domain, respectively and we study the dependence of the eigenvalues on the penalization parameter  $\alpha$ . From Proposition 1, the eigenvalues of problem (4) split

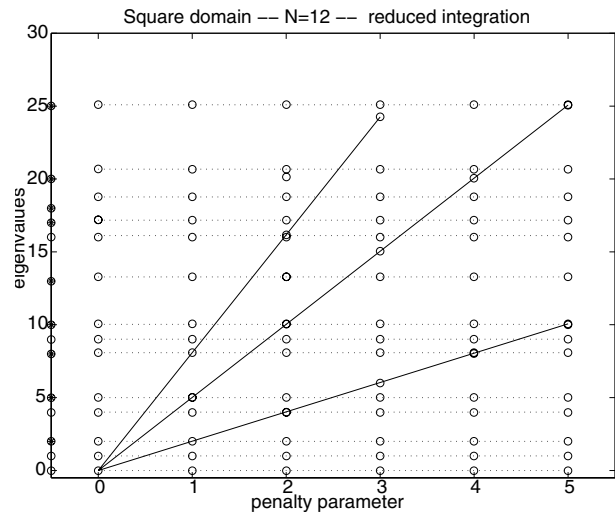
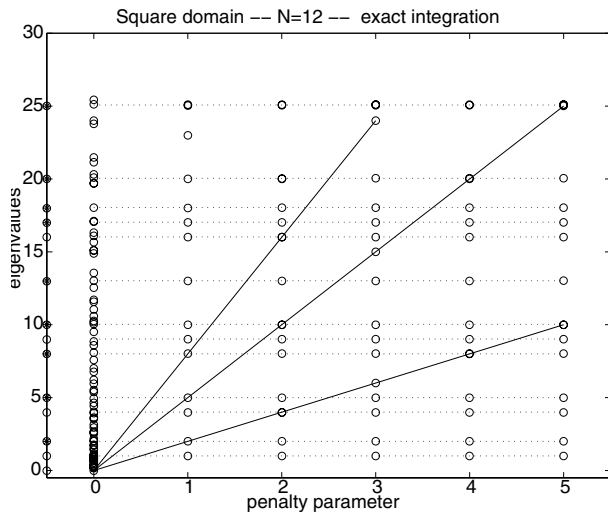
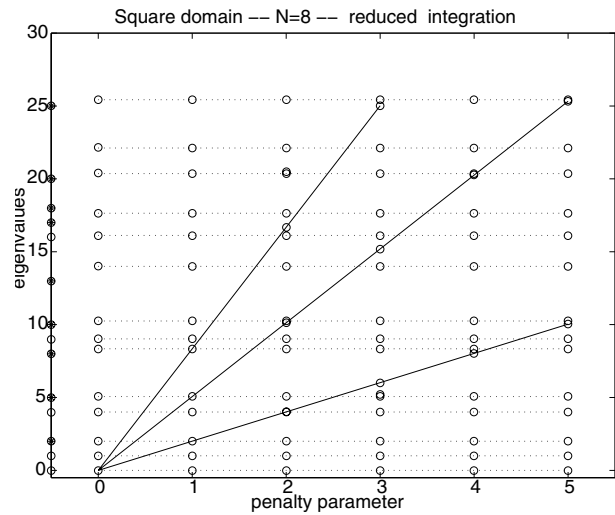
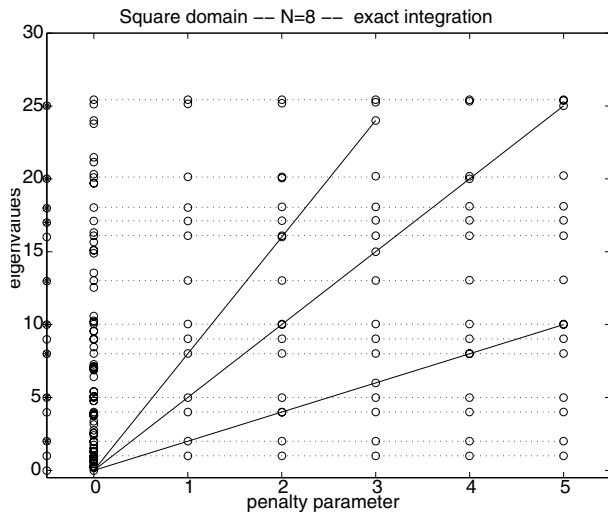


Figure 4 : Displacement-type approximation for square domain.

Figure 5 : Reduced integration approximation for square domain.

into two families: the first one independent of  $\alpha$ , the second one linearly dependent on  $\alpha$ . This splitting disappears when the  $H^1$  variational formulation (9) in a nonconvex domain is considered.

The numerical experiments show that the same behavior appears when the approximate problems (10) and (13) are considered in the case of convex domain, while for domains with reentrant corners the two formulations give completely different results.

As a first example we consider the domain  $\Omega = ]0, \pi[ \times ]0, \pi[$ . In this case the eigenvalues of problem (1) can be exactly evaluated:  $0 \neq \omega^2 = n^2 + m^2$ , with  $n, m = 0, 1, \dots$ . Let us subdivide the square  $\Omega$  into  $N^2$  squares of side  $h = \frac{\pi}{N}$ . In Fig. 4 we report the eigenvalues less than or equal to 25 when the penalty parameter varies from 1 to 5; they are obtained with the approx-

imation scheme (10) for two different meshes ( $N=8, 12$ ). The two expected families of eigenvalues appear. In order to help the reader we report on the y-axis the exact eigenvalues both of the Neumann problem (marked with a circle) and the Dirichlet one (marked with a star). The dotted lines join the eigenvalues of the first family. They lie on horizontal lines and coincide with the eigenvalues of the Neumann problem for the Laplace operator. The continuous lines join the eigenvalues of the second family; they depend linearly on  $\alpha$  and are multiple of the eigenvalues of the Dirichlet problem for the Laplace operator according to the relation (7). We observe that for  $\alpha = 0$  the well known phenomenon of spurious modes occurs. That is a number of positive discrete eigenvalues approximates badly the zero frequency and appears among the physically correct ones.

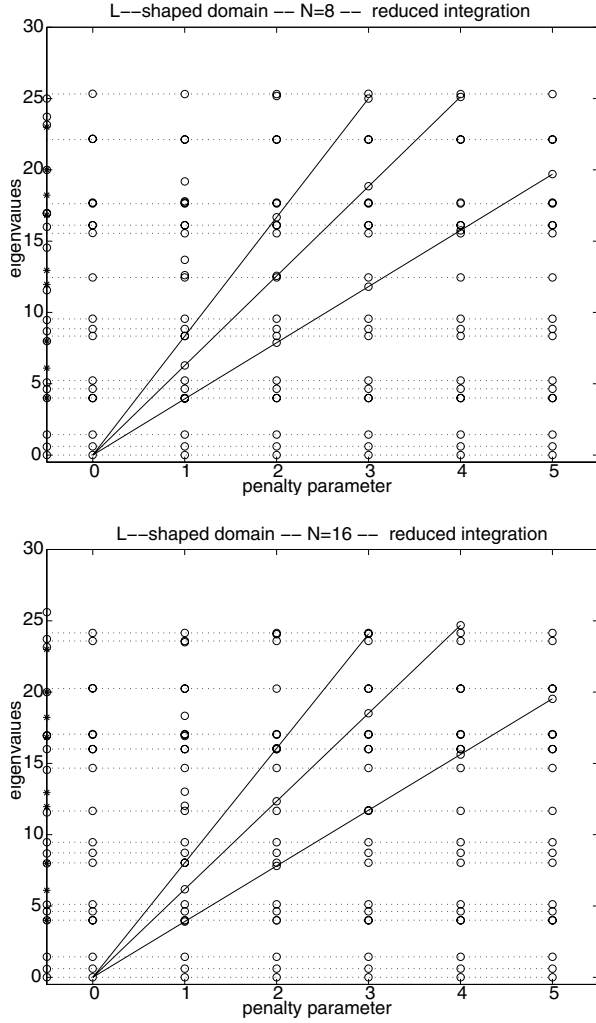


Figure 6 : Reduced integration scheme for L-shaped domain.

The eigenvalues obtained with the approximation scheme (13) are reported in Fig. 5. The same conclusions as for the previous scheme can be made. The only difference is for  $\alpha = 0$  since in this case no spurious modes occur. They appear all with zero frequency.

In the second example the domain is nonconvex and L-shaped:  $\Omega = \Omega_0 \setminus \Omega_1$ , where  $\Omega_0$  is the square with side  $\pi$ , like before, and  $\Omega_1$  is the square  $]0, \frac{\pi}{2}[ \times ]0, \frac{\pi}{2}[$ . Let us subdivide the domain  $\Omega$  into  $\frac{3}{4}N^2$  squares of side  $h = \frac{\pi}{N}$ , with  $N$  even.

In the first test we consider the approximation scheme (13) and as for the convex domain, we evaluate the eigenvalues less than or equal to 25 for  $\alpha$  ranging from 1 to 5. The eigenvalues obtained with this scheme, for  $N=8$  and 16, are reported in Fig. 6.

We observe that as in the case of the convex domain the eigenvalues split into two disjoint families. Moreover the singular eigenfunctions are well approximated. We consider the two

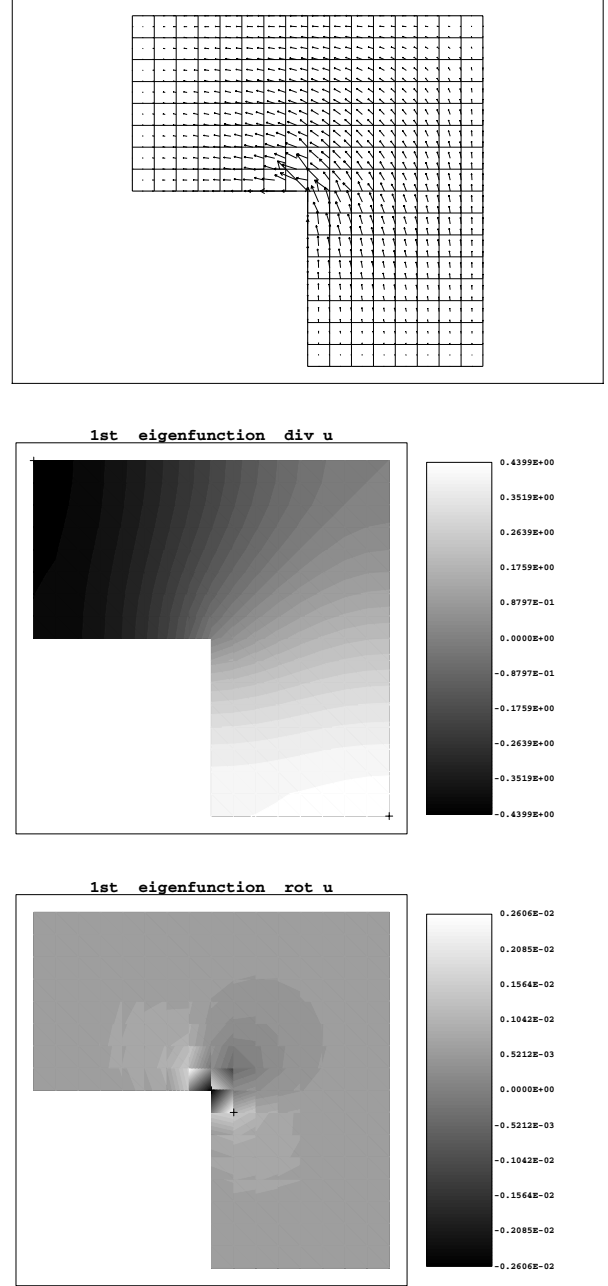
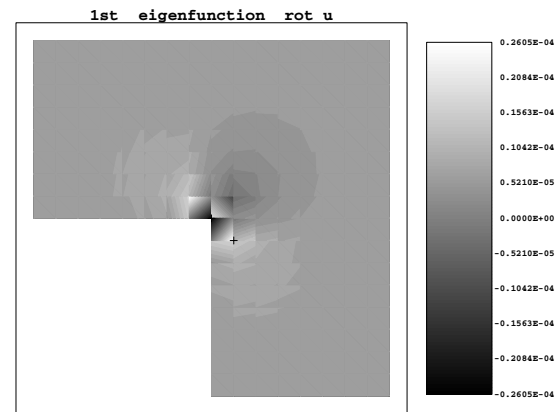
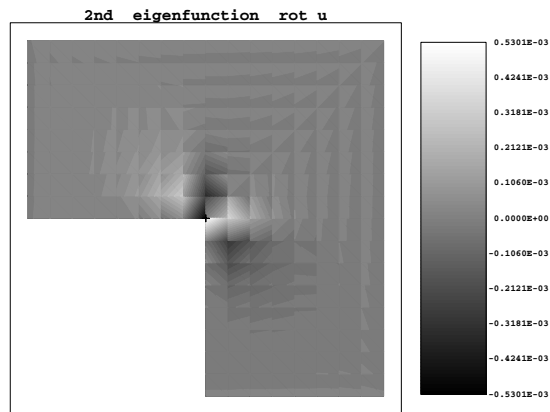
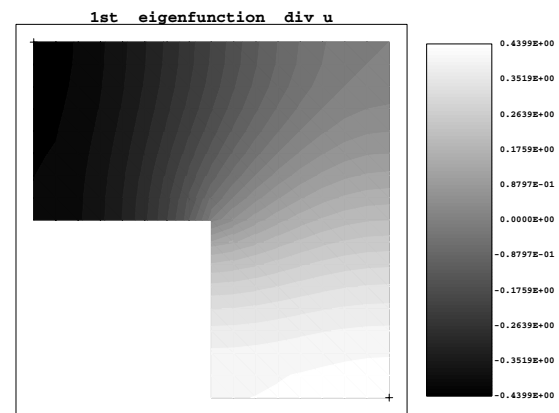
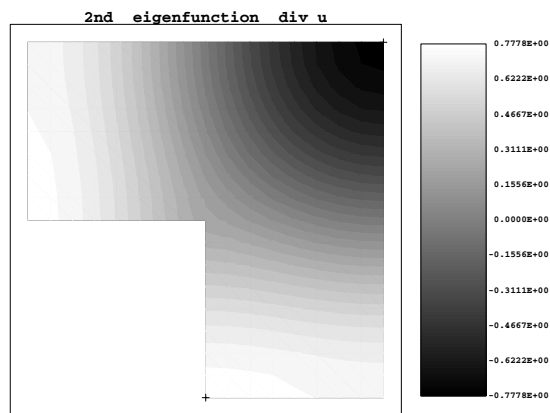
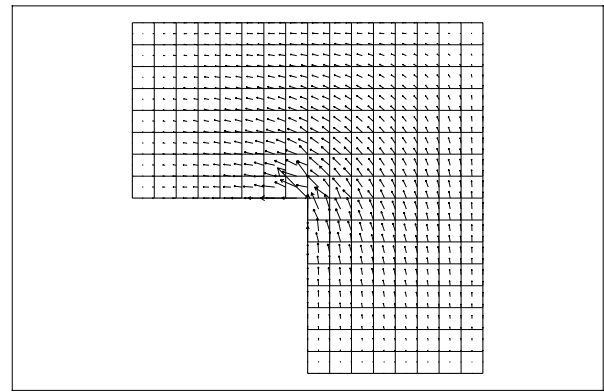
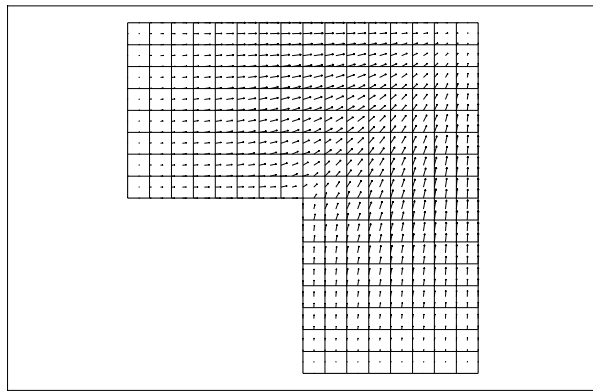


Figure 7 : Reduced integration scheme: 1st eigenfunction  $\alpha=1$

first eigenvalues: the first one is related to an eigenfunction with a singularity at the corner, while the second one is related to a regular eigenfunction. We evaluate the eigenfunctions, their divergences and their rotationals: the divergences represent the pressures of the fluid and the rotationals give a control on the irrotationality constraint. We consider a refined mesh ( $N=16$ ) and two different values of the penalty parameter ( $\alpha = 1$  and  $\alpha = 100$ ). In Fig. 7 we report the first eigenfunction with its pressure and rotational for  $\alpha = 1$ . In Fig. 8 the



**Figure 8** : Reduced integration scheme: 2nd eigenfunction  $\alpha=1$

**Figure 9** : Reduced integration scheme: 1st eigenfunction  $\alpha=100$

same quantities for the second eigenfunction in the case  $\alpha = 1$  are reported.

As expected the first computed eigenfunction tends to a singular eigenfunction, the second one is regular.

In Fig. 9 and 10 we report the same quantities for  $\alpha = 100$ . The pressures of both eigenfunctions are regular at the corner according to the  $H^1$ -regularity property (see Prop. 2) of the divergence of the solutions of problem (4). The rotationals tend

to zero, and seem to be  $H^1$ -regular according to the theoretical results. Moreover no differences appear in the eigenfunctions when the two different values of the penalty parameter are considered.

In the second test we consider the approximate scheme (10). In Fig. 11 we report the eigenvalues less than or equal to 10 for  $\alpha$  varying from 1 to 20, for  $N=8,16$ .



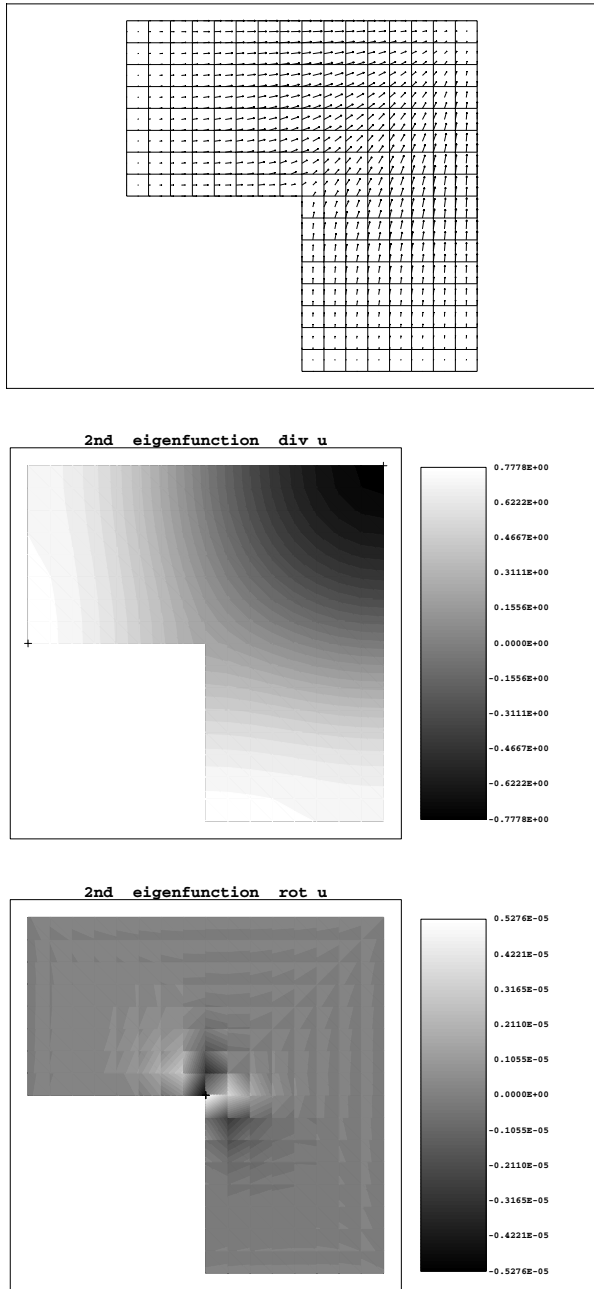


Figure 10 : Reduced integration scheme: 2nd eigenfunction  $\alpha=100$

Now three sets of eigenvalues appear: the eigenvalues joined with dotted lines, which coincide with the eigenvalues of the Neumann problem; the eigenvalues joined with continuous lines, which are multiples of the eigenvalues of Dirichlet problem and the eigenvalues joined with curved lines. These eigenvalues correspond to the  $H^1$ -eigensolutions of (9), which replace the singular solutions of problem (4). For small values of the penalty parameter the eigenvalues are ordered in the

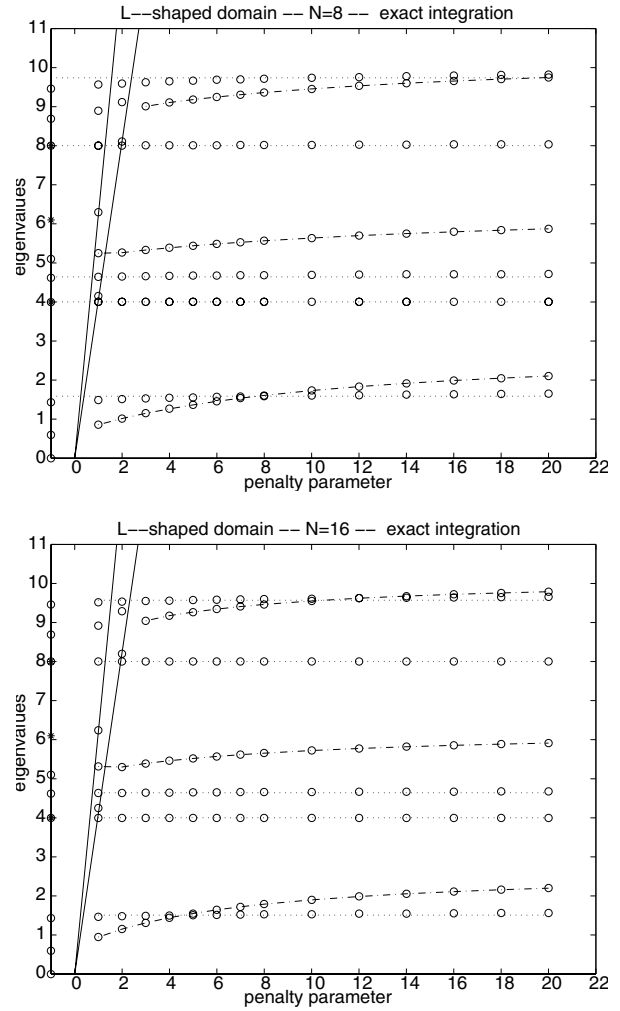
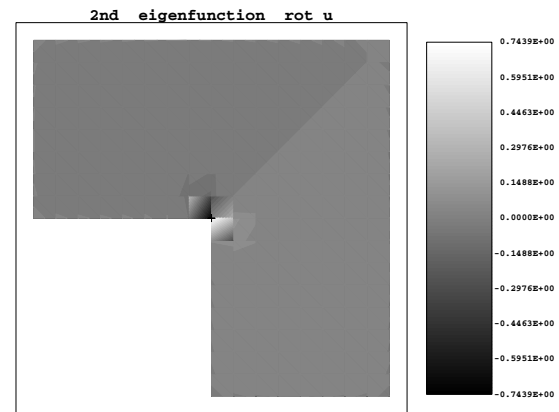
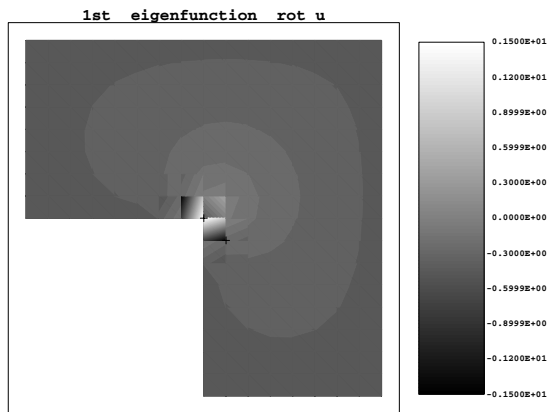
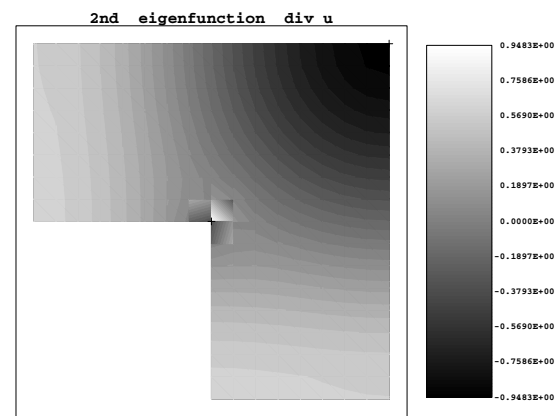
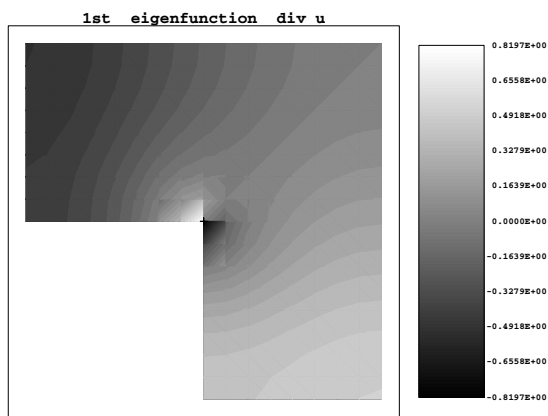
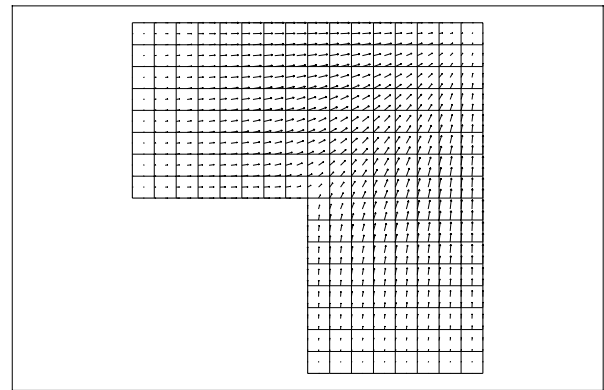
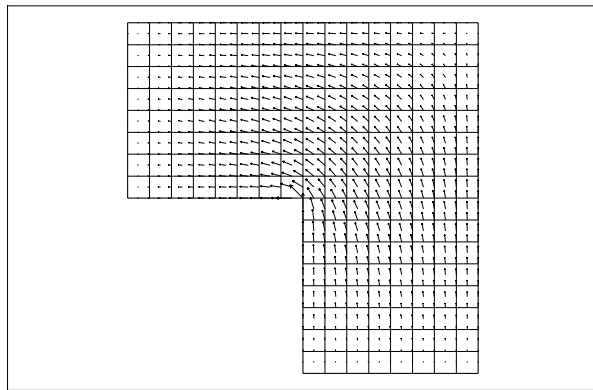


Figure 11 : Displacement-type approximation for L-shaped domain.

same way as those of problem (13). For example the first eigenvalue passes the second one for  $\alpha \geq 5$  and tends to a finite value when  $\alpha$  increases. In Fig. 12 and 13 we report the first and the second eigenfunction, respectively, for  $\alpha = 1$ . In Fig. 14 and 15 we report the same quantities for  $\alpha = 100$ . When the formulation (9) is used, we do not have the regularity result stated in Prop. 2. According to that, the pressures computed with the scheme (10) seem to be less regular than those obtained with the projection procedure (13). Moreover the first eigensolution for  $\alpha = 1$  becomes the second one for  $\alpha = 100$ . It tends to a regular function with zero value at the corner. In Fig. 16 we report the value of the first eigenfunction at the corner respect to the mesh size  $N$ , for different values of the penalty parameter both for the reduced and exact integration scheme. In the latter case the eigenfunction (as well as the corresponding eigenvalue) is changing as the penalty parameter increases and tends to zero at the corner.



**Figure 12** : Displacement-type approximation: 1st eigenfunction  $\alpha=1$

**Figure 13** : Displacement-type approximation: 2nd eigenfunction  $\alpha=1$

On the other hand in the former case the eigensolution is independent of the penalty parameter and depends only on the mesh refinement: when  $N$  increases its value at the corner gets bigger and the discrete eigenfunction approximates the singular solution.

Finally we evaluate the error  $E$  between the first three eigenvalues of the Neumann problem (5) and the corresponding

eigenvalues computed with the reduced integration procedure. In Fig.17 we plot, in *loglog* scale, the results obtained for  $\alpha = 100$  and for different meshes ( $N=4,8,16$ ). The slope of the lines allows an estimate of the order of convergence. As expected the first eigenvalue converges slower than the other two eigenvalues, since it corresponds to a singular eigenfunction.

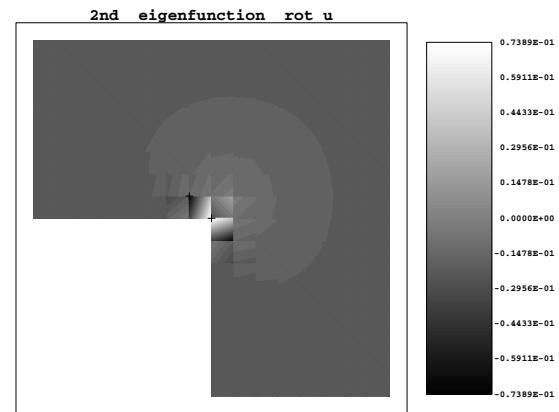
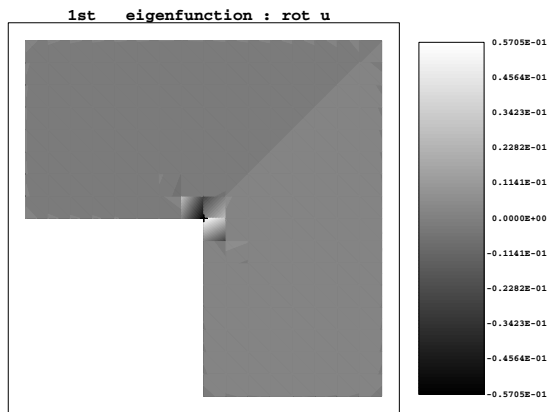
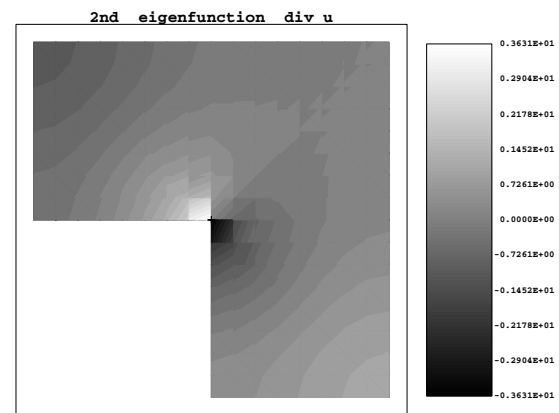
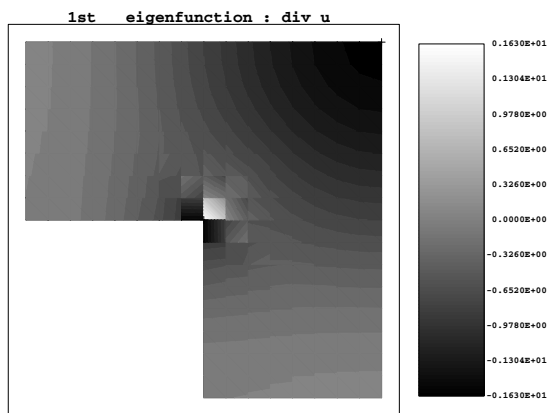
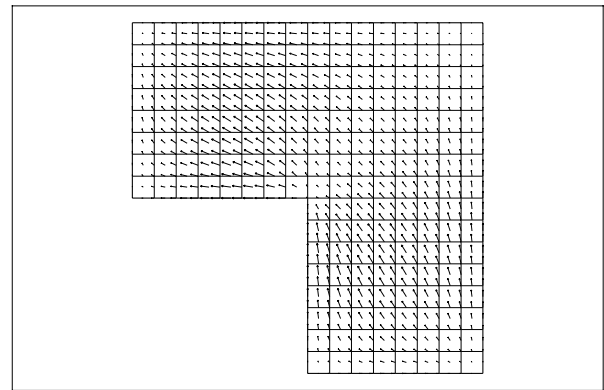
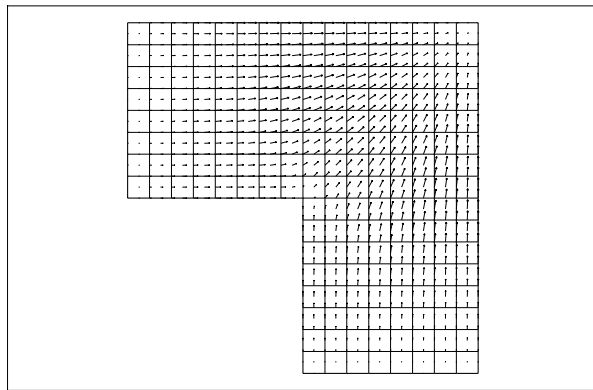


Figure 14 : Displacement-type approximation: 1st eigenfunction  $\alpha=100$

Figure 15 : Displacement-type approximation: 2nd eigenfunction  $\alpha=100$

**Acknowledgment**

This work has been partially supported by IAN-CNR, Pavia (Italy).

**References**

Bathe, K.-J.; Nitikitpaiboon, C.; Wang, X. (1995): A mixed displacement-based finite element formulation for

acoustic fluid-structure interaction. *Computers & Structures*, vol. 56, pp. 225–237.

Bermúdez, A.; Pedreira, D. (1992): Mathematical analysis of a finite element method without spurious solutions for computation of dielectric waveguides. *Numer. Math.*, vol. 61, pp. 39–57.

Bermúdez, I.; Durán, R.; Muschietti, A.; Rodríguez, R.;

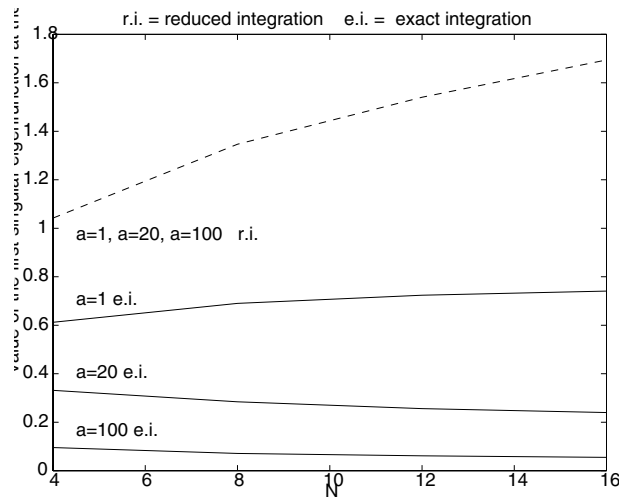


**Figure 16** : L-shaped domain: value of the first eigenfunction at the corner

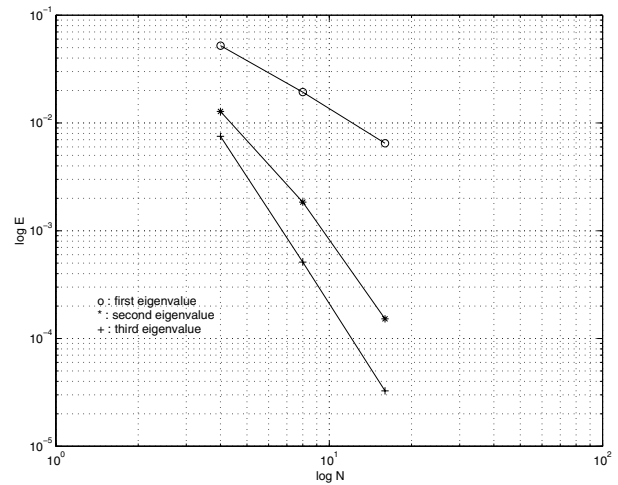


**Figure 17** : L-shaped domain, reduced integration scheme: relative error for the first three eigenvalues

**Solomin, J.** (1995): Finite element vibration analysis of fluid–solid systems without spurious modes. *SIAM J. Numer. Anal.*, vol. 32, pp. 1280–1295.

**Boffi, D.; Brezzi, F.; Gastaldi, L.** (1997): On the convergence of eigenvalues for mixed formulations. *Ann. Sc. Norm. Sup. Pisa*, vol. 25, pp. 131–154.

**Boffi, D.; Brezzi, F.; Gastaldi, L.** (1997): On the problem of spurious eigenvalues in the approximation of linear elliptic problems in mixed form. *Math. Comp.* to appear.

**Boffi, D.; Fernandes, P.; Gastaldi, L.; Perugia, I.** (1996): Edge approximation of eigenvalue problems arising from electromagnetics. In Désidéri; Tallec, L.; Oñate; Périaux; Stein(Eds): *Numerical Methods in Engineering '96*, pp. 551–556. Proceedings of the the Second ECCOMAS Conference, 9-13 September 1996, Paris, France, John Wiley & Sons.

**Boffi, D.; Fernandes, P.; Gastaldi, L.; Perugia, I.** (1999): Computational models of electromagnetic resonators: analysis of edge element approximation. *SIAM J. Numer. Anal.*, vol. 36, pp. 1264–1290.

**Bossavit, A.** (1990): Solving Maxwell equations in a closed cavity and the question of spurious modes. *IEEE Trans. on Magnetics*, vol. 26, pp. 702–705.

**Brezzi, F.; Fortin, M.** (1991): *Mixed and Hybrid Finite Element Methods*. Springer–Verlag, New York.

**Chen, H.; Taylor, R.** (1990): Vibration analysis of fluid–solid systems using a finite element displacement formulation. *Int. J. Numer. Methods Eng.*, vol. 29, pp. 683–698.

**Costabel, M.; Dauge, M.** (1997): Singularities of electromagnetic fields in polyhedral domains. *Arch. Rational Mech. Anal.* to appear.

**Costabel, M.; Dauge, M.** (1999): Maxwell and Lamé eigenvalues on polyhedra. *Math. Methods Appl. Sci.*, vol. 22, pp. 243–258.

**Gastaldi, L.** (1996): Mixed finite element methods in fluid structure systems. *Numer. Math.*, vol. 74, pp. 153–176.

**Kikuchi, F.** (1987): Mixed and penalty formulations for finite element analysis of an eigenvalue problem in electromagnetism. *Comput. Methods Appl. Mech. Eng.*, vol. 64, pp. 509–521.

**Morand; Ohayon** (1992): *Interactions fluides-structures*, volume RMA23 of *Recherches en mathématiques appliquées*. Masson, Paris.

**Nédélec, J.** (1982): Éléments finis mixtes incompressibles pour l'équation de Stokes dans  $\mathbf{R}^3$ . *Numer. Math.*, vol. 39, pp. 97–112.

**Raviart, P.-A.; Thomas, J.** (1977): A mixed finite element method for second order elliptic problems. In Galligani, I.; Magenes, E.(Eds): *Mathematical Aspects of the Finite Element Methods*, volume 606 of *Lecture Notes in Math.*, pp. 292–315, New York. Springer-Verlag.

**Wang, X.; Bathe, K.-J.** (1997): Displacement/pressure based mixed finite element formulations for acoustic fluid–structure interaction problems. *Int. J. Numer. Methods Eng.*, vol. 40, pp. 2001–2017.

**Wang, X.; Bathe, K.-J.** (1997): On mixed elements for acoustic fluid-structure interactios. *M<sup>3</sup>AS*, vol. 7, pp. 329–343.

**Webb, J.** (1993): Edge elements and what they can do for you. *IEEE Trans. on Magnetics*, vol. 29, pp. 1460–1465.

